Effects of strain in multiorbital superconductors: The case of Sr_2RuO_4

Sophie Beck,[1] Alexander Hampel,[1] Manuel Zingl,[1] Carsten Timm,[2,3] and Aline Ramires[4]
[1]*Center for Computational Quantum Physics, Flatiron Institute, 162 5th Avenue, New York, New York 10010, USA*
[2]*Institute of Theoretical Physics, Technische Universität Dresden, 01062 Dresden, Germany*
[3]*Würzburg-Dresden Cluster of Excellence ct.qmat, Technische Universität Dresden, 01062 Dresden, Germany*
[4]*Paul Scherrer Institute, CH-5232 Villigen PSI, Switzerland*

(Received 2 December 2021; revised 28 March 2022; accepted 30 March 2022; published 21 April 2022)

Uniaxial-strain experiments have become a powerful tool to unveil the character of unconventional phases of electronic matter. Here, we propose a combination of the superconducting fitness analysis and density functional theory calculations to dissect the effects of strain in complex multiorbital quantum materials from a microscopic perspective. We apply this framework to the superconducting state of Sr_2RuO_4 and argue that the recently proposed orbitally antisymmetric spin triplet order parameter candidate has unique signatures under strain which are in agreement with recent observations. In particular, we can account for the asymmetric splitting of the critical temperatures for compressive strain along the ⟨100⟩ direction and the reduction of the critical temperature for compressive strain along the ⟨001⟩ and ⟨110⟩ directions with a single free parameter.

DOI: 10.1103/PhysRevResearch.4.023060

I. INTRODUCTION

The recent development of strain devices suitable for a variety of experimental probes has opened a new direction of investigation of complex quantum materials [1]. The application of uniaxial strain along different directions allows for the selective reduction of spatial symmetries, which is key to uncovering the character of the underlying phases of matter in a variety of magnetic and superconducting materials [2–6]. Strain can tune material parameters such as orbital occupation [7], Fermi surface geometry [8], and topological properties [9]. Given the complexity of most of the functional materials available today, a clear understanding of the effects of strain from a microscopic perspective is highly desirable.

Here, we take as an example Sr_2RuO_4, a material whose superconducting order parameter has been the focus of debate for more than 25 years [10]. This system was recently investigated by thermodynamic [11,12], transport [13], angle-resolved photoemission spectroscopy (ARPES) [14], nuclear magnetic resonance (NMR) [15], and muon spin relaxation (μSR) [16] experiments under strain, giving us important hints on the nature of the superconducting state in this material.

The best contenders for the superconducting state of Sr_2RuO_4 are chiral order parameters [17–20]. Chiral superconductivity is supported by several experimental probes: Polar Kerr rotation experiments reveal time-reversal symmetry breaking (TRSB) at the superconducting critical temperature T_c [21], ultrasound attenuation experiments indicate a two-component order parameter [22–24], and the study of junctions suggest the presence of superconducting domains [25,26]. Also, recent μSR measurements under compressive strain along the ⟨100⟩ direction show a clear splitting between the superconducting critical temperature T_c and the temperature below which TRSB is observed (T_{TRSB}) [16]. A splitting is expected for a chiral superconductor, but some of the features observed experimentally cannot be accounted for by a simple phenomenological Ginzburg-Landau theory. First, the transition seems to be rather asymmetric concerning the evolution of the two temperatures: T_c is strongly enhanced, while T_{TRSB} remains almost unchanged up to uniaxial strains of about 1% [16]. Second, the evolution of T_c is strongly nonlinear, and there is no observable cusp of T_c around zero strain [11]. In addition, recent experiments indicate that compressive strain along the ⟨001⟩ direction causes a reduction of T_c [27]. This behavior is in contradiction with the expected enhancement based on a weak-coupling scenario with an increased density of states (DOS) given the proximity to the van Hove singularity. Furthermore, experiments under compressive strain along the ⟨110⟩ direction indicate a mild suppression of the critical temperature [28].

The original proposal of a chiral superconducting state for Sr_2RuO_4 suggested a p-wave triplet state with $\mathbf{d}$-vector along the z-direction [17]. This state is hard to reconcile with new NMR experiments [15]: The reduction of the Knight shift for in-plane fields is expected only for singlet or triplet states with an in-plane d-vector. Furthermore, the standard chiral p-wave state has difficulties accounting for thermodynamic [29] and transport [30] experiments indicating the presence of gap nodes. In this context, some of us recently proposed a new order parameter candidate: An even-parity pseudospin-singlet chiral superconducting state with horizontal line nodes [31]. In the microscopic orbital basis, this superconducting state

in the E_g channel is an s-wave orbital-antisymmetric spin triplet (OAST), which can be stabilized by local interactions in the presence of a large effective Hund coupling and realistic three-dimensional spin-orbit coupling [31].

Here, we investigate the effects of strain on a local order parameter with E_g symmetry. We conclude that the concept of *superconducting fitness* [32–35] in conjunction with density functional theory (DFT) calculations can clarify the origin of the unusual features of the evolution of T_c and T_{TRSB} under strain along different directions in a consistent manner. For that, we use the evolution of the normal state band structure from DFT and a single free parameter. Our analysis stems from a microscopic perspective and captures qualitatively new effects beyond a naive Ginzburg-Landau construction. In particular, we discuss the microscopic origin of the asymmetry of T_c and T_{TRSB} under strain along the $\langle 100\rangle$ direction, and how strain along the $\langle 001\rangle$ direction reduces T_c, even though the DOS is enhanced. Moreover, we discuss the behavior of the transition temperatures under strain along the $\langle 110\rangle$ direction.

II. THEORETICAL DESCRIPTION

The simplest form of superconducting fitness measures was introduced in the context of two-orbital models [34]. To apply this framework to the analysis of strain effects in Sr_2RuO_4, we need to simplify the standard three-orbital model based on the d_{xz}, d_{yz}, and d_{xy} orbitals. Given the recently acknowledged importance of the k_z direction [31], we consider projections of the three-orbital model into the k_xk_z and k_yk_z planes (from now on we refer to these planes as XZ and YZ, respectively). In these planes, only two Fermi surfaces are present: The γ band, composed mostly of d_{xy} orbitals, and the β band, composed primarily of d_{xz} and d_{yz} orbitals, as shown in Fig. 1. In particular, in the XZ (YZ) plane the Fermi surfaces are primarily formed by d_{xz} (d_{yz}) and d_{xy} orbitals. We are then able to construct effective two-orbital models for the electronic structure along these planes. Note that the models in the XZ and YZ planes are not the same, the first is a model for d_{xz} and d_{xy} orbitals, while the second is a model for d_{yz} and d_{xy} orbitals. Note also that the density of states and its change under strain are higher in these planes, compared to other planes containing the k_z axis. Furthermore, the order parameter of interest here has gap maxima in these planes and gap minima along the diagonals [31,35], suggesting that the XZ and YZ planes are indeed the most important for superconductivity in this scenario. Considering both planes together, we believe our approach captures the essential physics of the three-orbital three-dimensional model for Sr_2RuO_4.

The reduced models along the XZ and YZ planes have D_{2h} point group symmetry, within which we find only one-dimensional irreducible representations (irreps). At first sight, it seems that we have lost the discussion about the splitting of the degenerate superconducting transitions in E_g for the complete model with D_{4h} symmetry. Here, the reduced models along the XZ and YZ planes should be seen as degenerate. Their inequivalence under strain is a manifestation of the symmetry breaking.

For concreteness, here we consider the XZ plane, dominated by the d_{xz} and d_{xy} orbitals. Projecting into this subspace,

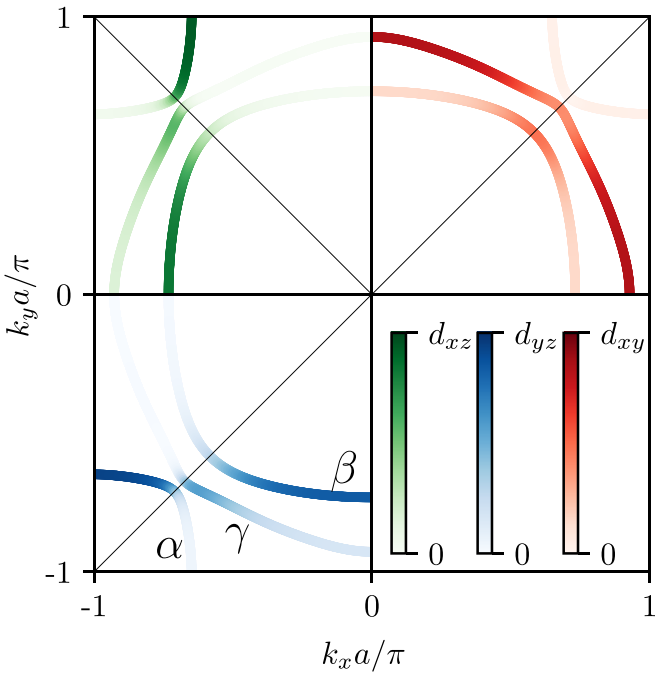

FIG. 1. Fermi surfaces indicating the orbital distribution for unstrained Sr_2RuO_4 in the $k_z = 0$ plane. The color red (blue, green) encodes the orbital d_{xy} (d_{yz}, d_{xz}) content as low (bright) or high (dark) color in each Fermi surface sheet. The data are obtained by combining the *ab initio*-derived tight-binding Hamiltonian with a local correlation-enhanced effective spin-orbit coupling term ($\lambda = 0.2$ eV) [51].

we obtain the following effective two-orbital Hamiltonian:

$$\mathcal{H}_0^{XZ} = \sum_{\mathbf{k}} \Psi_{\mathbf{k}}^\dagger \hat{H}_0^{XZ}(\mathbf{k}) \Psi_{\mathbf{k}}, \tag{1}$$

in the basis $\Psi_{\mathbf{k}}^\dagger = (c_{\mathbf{k},xz\uparrow}^\dagger, c_{\mathbf{k},xz\downarrow}^\dagger, c_{\mathbf{k},xy\uparrow}^\dagger, c_{\mathbf{k},xy\downarrow}^\dagger)$, with

$$\hat{H}_0^{XZ}(\mathbf{k}) = \sum_{a,b=0}^{3} \tilde{h}_{ab}^{XZ}(\mathbf{k})\, \hat{\tau}_a \otimes \hat{\sigma}_b, \tag{2}$$

where the $\tilde{h}_{ab}^{p}(\mathbf{k})$ are real even functions of momentum labeled by indexes $(a,b)_p$, with a and b corresponding to $\hat{\tau}_a$ and $\hat{\sigma}_b$, the Pauli matrices encoding the orbital and the spin degrees of freedom, respectively ($\hat{\sigma}_0$ and $\hat{\tau}_0$ are identity matrices), and $p = \{XZ, YZ\}$ corresponds to the plane. There are, in principle, 16 functions labeled as $(a,b)_{XZ}$, but in the presence of time-reversal and inversion symmetries these are constrained to only six: $(0,0)_{XZ}$, $(3,0)_{XZ}$, and $(2,1)_{XZ}$ in A_g, the first two associated with intraorbital hopping and the last with atomic spin-orbit coupling (SOC); $(2,2)_{XZ}$ in B_{1g} and $(2,3)_{XZ}$ in B_{2g}, both associated with momentum-dependent SOC; and $(1,0)_{XZ}$ in B_{3g} associated with interorbital hopping. Analogously, we parametrize the local gap matrices in the orbital basis as

$$\hat{\Delta}^{XZ} = d_0\, \hat{\tau}_a \otimes \hat{\sigma}_b\, (i\hat{\sigma}_2), \tag{3}$$

where d_0 is the order parameter amplitude. A similar construction holds for the YZ plane. The derivation of the terms in the normal state Hamiltonian, labeled as $(a,b)_p$, and order param-

eters, labeled as $[a, b]_p$, are given in detail in the Supplemental Material (SM) [36], which also includes Refs. [37–50].

From here on, we focus on the even parity OAST order parameter proposed in Ref. [31]. This is a two-component order parameter with E_g symmetry, which reconciles several experimental observations. In the complete description of Sr_2RuO_4 as a three-dimensional three-orbital model (see details in the SM [36]), the order parameter is dominated by the basis matrices {[5, 3], [6, 3]}. Once we project the complete model into the XZ or YZ planes, we identify the order parameters as follows:

$$[5, 3] \to [2, 3]_{YZ}, \tag{4}$$

$$[6, 3] \to [2, 3]_{XZ}. \tag{5}$$

The Gell-Mann matrices $\hat{\lambda}_5$ and $\hat{\lambda}_6$ are 3×3 antisymmetric matrices carrying information about the orbital combination in the superconducting order parameter. Once projected onto the two-orbital models, both components of the order parameter are associated with the Pauli matrix $\hat{\tau}_2$, the only antisymmetric 2×2 matrix. Note that for [5,3] and $[2, 3]_{YZ}$, the pairing is between d_{yz} and d_{xy} orbitals, whereas for [6,3] and $[2, 3]_{XZ}$ the pairing is between d_{xz} and d_{xy} orbitals. The quantitative analysis below is done within the two-orbital models, and we use the correspondences above to connect the results to the original three-orbital problem with D_{4h} symmetry.

Within the standard weak-coupling assumptions, the superconducting critical temperature for a two-orbital system under strain can be written as [34]

$$T_c(s) \approx \frac{4e^{\gamma}}{\pi}\frac{\omega_C}{2}\exp\left[\left(-\frac{1}{2|v|} - \delta(s)\right)\frac{1}{\alpha(s)}\right], \tag{6}$$

where γ is the Euler constant, ω_C is a characteristic energy cutoff, $|v|$ is the magnitude of the attractive interaction in the symmetry channel of interest (the last two assumed to be strain independent). The superconducting fitness functions are written as

$$\alpha(s) = \frac{1}{16}\sum_a N_a(0, s)\langle||\hat{F}_A(\mathbf{k}_{Fa}, s)||^2\rangle_{\mathrm{FS}_a}, \tag{7}$$

and

$$\delta(s) = \frac{\omega_C^2}{32}\sum_a N_a(0, s)\left\langle\frac{||\hat{F}_C(\mathbf{k}_{Fa}, s)||^2}{q(\mathbf{k}_{Fa})^2}\right\rangle_{\mathrm{FS}_a}, \tag{8}$$

where $q(\mathbf{k}) = \epsilon_a(\mathbf{k}) - \epsilon_b(\mathbf{k})$ is the energy difference between the two bands. The index a corresponds to the distinct Fermi surfaces with DOS $N_a(0, s)$ at the Fermi level for strain s, and $\langle\ldots\rangle_{\mathrm{FS}_a}$ indicates the average over the respective Fermi surface. $||\hat{M}||^2 = \mathrm{Tr}[\hat{M}\hat{M}^{\dagger}]$ is the Frobenius norm of the matrix $\hat{M}$. The superconducting fitness matrices are defined as

$$\hat{F}_{A,C}(\mathbf{k}, s)(i\hat{\sigma}_2) = \tilde{H}_0(\mathbf{k}, s)\tilde{\Delta}(\mathbf{k}) \pm \tilde{\Delta}(\mathbf{k})\tilde{H}_0^*(-\mathbf{k}, s), \tag{9}$$

where $\tilde{H}_0(\mathbf{k}, s) = [\hat{H}_0(\mathbf{k}, s) - \tilde{h}_{00}(\mathbf{k}, s)\hat{\sigma}_0 \otimes \hat{\tau}_0]/|\tilde{h}(\mathbf{k}, s)|$, with $|\tilde{h}(\mathbf{k}, s)|^2 = \sum_{(a,b)\neq(0,0)}|\tilde{h}_{ab}(\mathbf{k}, s)|^2$, is the normalized normal state Hamiltonian and $\tilde{\Delta}(\mathbf{k}) = \hat{\Delta}(\mathbf{k})/d_0$ is the normalized gap matrix. The index C (A) in $\hat{F}_{C(A)}(\mathbf{k}, s)$ corresponds to the (anti)commutator nature of this quantity. A finite $\hat{F}_A(\mathbf{k}, s)$ corresponds to the weight of intraband pairing, guaranteeing a robust weak coupling instability. Conversely, a finite $\hat{F}_C(\mathbf{k}, s)$ corresponds to the weight of interband pairing, which is detrimental to the superconducting instability and reduces the critical temperature.

III. RESULTS AND DISCUSSION

For small strain, we can determine the evolution of the superconducting fitness functions using the evolution of the hopping amplitudes and the total DOS evaluated by DFT calculations (see SM [36] for quantitative estimates). Given the proximity of the two Fermi surfaces at the XZ and YZ planes, we assume that the superconducting fitness functions for each Fermi surface are going to be approximately the same. We define

$$\langle||\hat{F}_A(\mathbf{k}, s)||^2\rangle \approx \langle||\hat{F}_A(\mathbf{k}, 0)||^2\rangle(1 + F_1 s + F_2 s^2), \tag{10}$$

for a representative Fermi vector and the total density of states

$$N(0, s) \approx N(0, 0)(1 + N_1 s + N_2 s^2). \tag{11}$$

The coefficients $F_{1,2}$ and $N_{1,2}$ are summarized in Table I for compressive strain along different directions.

To get a simpler form for the evolution of the critical temperature with strain, we use the relation $||\hat{F}_A(\mathbf{k})||^2 + ||\hat{F}_C(\mathbf{k})||^2 = 4$ and write

$$\alpha(s) \approx \alpha(0)(1 + N_1 s + N_2 s^2)(1 + F_1 s + F_2 s^2), \tag{12}$$

$$\delta(s) \approx \delta(0)(1 + N_1 s + N_2 s^2)[1 - A(F_1 s + F_2 s^2)], \tag{13}$$

where $A = \langle||\hat{F}_A(0)||^2/q^2\rangle_{\mathrm{FS}a}/\langle||\hat{F}_C(0)||^2/q^2\rangle_{\mathrm{FS}a}$, with an implicit $\mathbf{k}$ dependence. For the $[2, 3]_{XZ/YZ}$ order parameters, we estimate $A \approx 10^{-5}$, (see quantitative discussion in the SM [36]). The small value of A allows us to neglect the dependence of $\delta(s)$ on strain through the $F_{1,2}$ coefficients. Furthermore, within the assumption that $1 \gg 2|v|\delta(0)$, we

TABLE I. Coefficients for the evaluation of the evolution of the critical temperature as a function of strain for the {[5, 3], [6, 3]} order parameter inferred from the analysis of the two-orbital models along the XZ and YZ planes. N_1 and N_2: Coefficients determining the evolution of the density of states at the Fermi energy. F_1 and F_2: Coefficients determining the evolution of $||\hat{F}_A(\mathbf{k}, s)||^2$, as in Eq. (10), obtained by selecting a representative $k_F = 2.67$ to be between the β and γ Fermi surfaces. Note that compressive strain correspond to negative values.

Direction	SC Component	$N_1(\%s)^{-1}$	$N_2(\%s)^{-2}$	$F_1(\%s)^{-1}$	$F_2(\%s)^{-2}$
⟨100⟩	[5,3]	−0.0928	+0.4143	+0.0333	−0.0125
	[6,3]	+0.2536	+0.0797	−0.0091	−0.0042
⟨001⟩	{[5, 3], [6, 3]}	−0.0503	+0.0072	+0.0589	−0.0024
⟨110⟩	{[5, 3], [6, 3]}	+0.0296	+0.0074	+0.0129	−0.0004

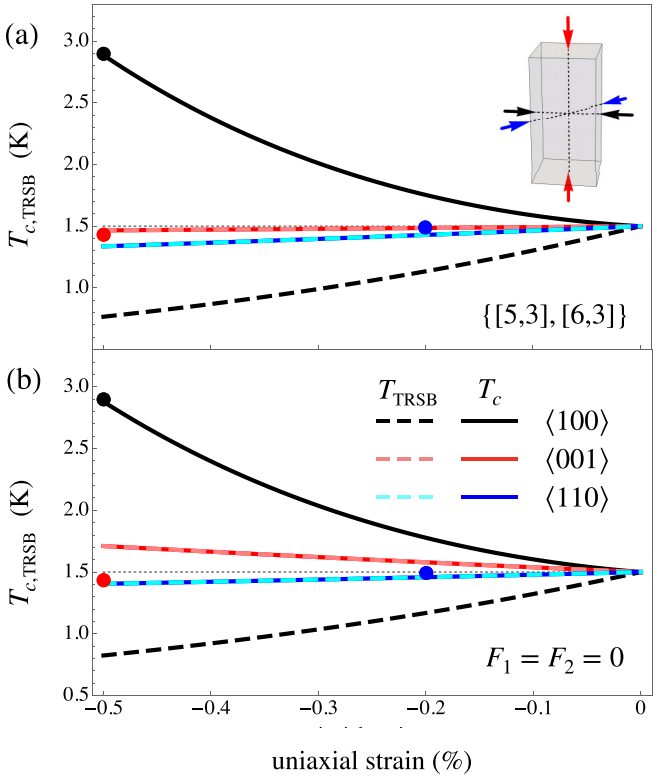

FIG. 2. Evolution of T_c and T_{TRSB} under compressive uniaxial strain along the ⟨100⟩, ⟨001⟩, and ⟨110⟩ directions for the order parameter {[5, 3], [6, 3]}, (a) with $g = 5.8$ and (b) setting $F_1 = F_2 = 0$ for $g = 5$. The horizontal dotted line is a guide to the eye corresponding to the unstrained critical temperature. The black and red (blue) circles at $s = -0.5\%$ ($s = -0.2\%$) correspond to the experimental value for strain along the ⟨100⟩ and ⟨001⟩ (⟨110⟩) directions obtained from Refs. [12,27] ([28]), respectively. We took the Young's modulus along the ⟨001⟩ direction to be approximately 200 GPa. For both plots we set the representative $k_F = 2.67$ to be between the β and γ Fermi surfaces.

take $\delta(s) \approx \delta(0)$, such that the dependence of the critical temperature on strain is carried only by the fitness function $\alpha(s)$. Within these considerations, the closed form equation for the evolution of T_c can be cast as

$$\frac{T_c(s)}{T_c(0)} \approx \exp\left[g\left(1 - \frac{\alpha(0)}{\alpha(s)}\right)\right], \tag{14}$$

where $g = [1/(2|v|) + \delta(0)]/\alpha(0)$, the only free parameter in this analysis, is chosen such that our results are in good agreement with the experimentally observed value of $T_c(s = -0.5\%) \approx 2.9$ K for strain along the ⟨100⟩ direction [12]. Our results for strain along different directions are summarized in Fig. 2. Note that for strain along the ⟨100⟩ direction, the transition temperatures for $[2, 3]_{XZ}$ and $[2, 3]_{YZ}$ evolve differently, indicating the splitting of the two originally degenerate components {[5, 3], [6, 3]} in E_g. We associate the higher temperature with T_c and the lower temperature with T_{TRSB}. As expected, for strain along the ⟨001⟩ direction T_c and T_{TRSB} are the same as there is no symmetry breaking. Finally, for strain along the ⟨110⟩ direction there is symmetry breaking, but its effect cannot be captured by our approach. Here we consider only the XZ and YZ planes, which remain equivalent under strain along the ⟨110⟩ direction. Only directions away from the zone axes can capture the symmetry breaking (see further discussion in the SM [36]).

To qualitatively understand the evolution of the critical temperatures as a function of strain along different directions, we summarize here some of the properties of the parameters in the normal state Hamiltonian along the XZ plane. The dominant term within $(3, 0)_{XZ}$ is associated with the imbalance in the intraorbital nearest-neighbor hopping amplitudes for the d_{xz} and d_{xy} orbitals. $(2, 1)_{XZ}$ is associated with the correlation-enhanced effective atomic SOC, taken as $\eta \approx 0.2$ eV [51]. $(2, 3)_{XZ}$ is associated with momentum-dependent SOC in the B_{2g} irrep. As an estimate, here we take its value to be equal to one-tenth the hopping amplitude with the same interorbital structure [31], $t^{\mathrm{SOC}}_{xy/xz}(\hat{d}_d) \approx t_{xy/xz}(\hat{d}_d)/10 \approx 0.68$ meV. By symmetry, $(2, 2)_{XZ}$ and $(1, 0)_{XZ}$ are zero along the XZ plane. We then focus on the evolution of the terms $(3, 0)_{XZ}$ and $(2, 3)_{XZ}$ with strain. The analysis for the YZ plane leads to a similar conclusion. The evolution of the hopping amplitudes and DOS as a function of strain is determined by DFT calculations, performed without SOC. The correlation-enhanced effective atomic SOC is taken by its agreement with the experimental Fermi surfaces [51] and was verified not to change significantly with strain (this result will be published elsewhere).

For compressive strain along the ⟨100⟩ direction, we see from Table I that the dominant coefficients defining the evolution of the critical temperature with strain are associated with the evolution of the DOS ($|N_{1,2}| > |F_{1,2}|$). The effect of the fitness measure $||\hat{F}_A(\mathbf{k}, s)||^2$ is simply to slow down the evolution of the critical temperatures, as $F_{1,2}$ and $N_{1,2}$ have opposite sign. To note here is that at the linear level the evolution of the DOS, and therefore of the critical temperatures, is already rather asymmetric. Furthermore, for the [5,3] component there is a very large quadratic contribution to the evolution of the DOS due to the proximity to a van Hove singularity, which reflects on the evolution of the critical temperature, as shown in Fig. 2(a) (black curve). Given these coefficients obtained for low strain, we would expect an upturn of T_{TRSB} for $s = -1.7\%$. While this is a relatively high strain value, the upturn can be accessed in experiments by deviations from linear behavior at low strains.

Compressive strain along the ⟨001⟩ direction does not reduce the symmetry group, and as a consequence there is no splitting of the superconducting transition temperatures. For this strain direction, we find $|F_1| > |N_1|$, which indicates that the behavior of the critical temperature as a function of strain is dominated by the evolution of the superconducting fitness measure $||\hat{F}_A(\mathbf{k}, s)||^2$. This is in contrast to the discussion above for strain along the ⟨100⟩, with the evolution of the critical temperature dominated by the DOS. To understand the evolution of the fitness measure under compressive strain, we can look more carefully at how each term in the normal state Hamiltonian evolves with strain. The superconducting fitness analysis tells us that, for the order parameter $[2, 3]_{XZ}$, the normal state term $(3, 0)_{XZ}$ contributes to a finite $\hat{F}_C(\mathbf{k})$ and $(2, 3)_{XZ}$ contributes to a finite $\hat{F}_A(\mathbf{k})$. For compressive strain along the ⟨001⟩ direction, the magnitude of $(3, 0)_{XZ} \propto t_{xz}(\hat{x}) - t_{xy}(\hat{x})$ [here $t_\gamma(\hat{n})$ stands for the intraorbital hopping

amplitude for orbital γ along the $\hat{n}$ direction] is enhanced, leading to an increase of $\hat{F}_C(\mathbf{k})$, and $(2,3)_{XZ}$ is reduced, leading to a reduction in $\hat{F}_A(\mathbf{k})$, such that the coefficient F_1 is positive (compressive strain corresponds to negative values). Interestingly, at the quadratic level the evolution of the critical temperature is dominated by the DOS, as $|N_2| > |F_2|$ and we predict an upturn of the critical temperature for strain values of approximately -2.2%. The results for the $\langle 001\rangle$ direction are shown in Fig. 2(a) (red and pink curves).

We also consider the behavior of the critical temperatures under compressive strain along the $\langle 110\rangle$ direction. Strain along this direction reduces the point group symmetry, but as we are modeling only the XZ and YZ planes, we cannot capture the symmetry breaking and our results show the same strain evolution for both critical temperatures. In this case the behavior is dominated by the evolution of the DOS, this time in agreement with the evolution of the superconducting fitness function at the linear level. We observe an overall reduction of the critical temperature for both components. These results are summarized in Fig. 2(a) (blue and cyan curves). For this direction an upturn of the critical temperatures would also be expected for $s \approx -2.9\%$. In a more complete treatment with a three-dimensional Fermi surface, we expect to see a splitting of the critical temperatures away from the line we have currently obtained. This suggests that if the splitting is smaller than the absolute reduction of the critical temperatures we have observed here, both T_c and T_{TRSB} could be suppressed as a function of compressive strain, as preliminary experimental results indicate [52].

To highlight the effects of the fitness parameters, we show the evolution of T_c and T_{TRSB} in Fig. 2(b) when the coefficients in Eq. (10) are set to zero by hand, $F_1 = F_2 = 0$. Then the evolution of the critical temperature is controlled only by the evolution of the DOS through the coefficient $N_{1,2}$ in Table I. Note that although the behavior for strain along the $\langle 100\rangle$ direction is similar to the $\{[5,3],[6,3]\}$ scenario (black curves) with a slightly different value of g, compressive strain along the $\langle 001\rangle$ direction leads to an enhancement of T_c (red and pink curves), while strain along the $\langle 110\rangle$ reduces the critical temperature (blue and cyan curves).

We emphasize that the consistent account of the reduction of the critical temperature for compressive strain along the $\langle 001\rangle$ and $\langle 110\rangle$ directions and the enhancement of the critical temperature for compressive strain along the $\langle 100\rangle$ direction seems to be a unique feature of the recently proposed OAST superconducting state with E_g symmetry dominated by $\{[5,3],[6,3]\}$. From a naive weak-coupling scenario, it is very hard to account for a reduction in T_c under strain along the $\langle 001\rangle$ direction and an increase in T_c under strain along the $\langle 100\rangle$ direction given the enhancement of the DOS under compression in both cases, as recently discussed in Refs. [27,53].

At this point we would like to highlight that the phenomenology of the proposed OAST superconducting state is in agreement with multiple other experimental probes. In particular, the OAST order parameter is in agreement with recent NMR measurements [15]. Note that the order parameter is a spin-triplet in the orbital basis but it is a pseudospin-singlet in the band basis, consistent with even parity. The low-energy response to a magnetic field is then consistent with the one observed for spin-singlet superconductors. This has been numerically studied for similar pairing states in Refs. [54]. 'These studies have shown that only a small fraction of the normal-state spin susceptibility persists at zero temperature in the superconducting state. Other key experiments are polarized Kerr effect [21] and muon spin resonance [16], which indicate time-reversal symmetry breaking below T_c. In conjunction with recent ultrasound attenuation experiments suggesting a multi-component order parameter [22,55], a chiral superconducting state is one of the most natural contenders. A very recent experimental compilation [16] on the behavior of T_c under hydrostatic pressure and for different levels of disorder provides independent support for a superconducting state with two components related by symmetry, therefore associated with a two-dimensional irreducible representation.

IV. CONCLUSION

In conclusion, this work proposes a microscopic perspective for the understanding of the effects of strain in superconductors with multiple degrees of freedom based on the superconducting fitness analysis. This construction is particularly useful to go beyond the predictions of effective Ginzburg-Landau theories. Assuming an OAST superconducting state with E_g symmetry, we are able to account for the evolution of the critical temperatures under strain along three different directions with a single free parameter g, associated with the strength of the interactions. In particular, we find that compressive strain along the $\langle 100\rangle$ direction can lead to an asymmetric splitting of T_c and T_{TRSB}, and that compressive strain along the $\langle 001\rangle$ direction reduces T_c, even though the DOS at the Fermi surface is enhanced. We also find that up to splitting, both T_c and T_{TRSB} are reduced under compressive strain along the $\langle 110\rangle$ direction. These results indicate that the phenomenology of the OAST order parameter satisfies important constraints imposed by recent experiments. We believe that this kind of analysis can be extremely useful for understanding the behavior of other complex superconductors under strain and to ultimately determine the symmetry of the superconducting order parameter in these materials.

ACKNOWLEDGMENTS

The authors would like to thank S. Ghosh, V. Grinenko, C. Hicks, F. Jerzembeck, and H.-H. Klauss for interesting discussions. The Flatiron Institute is a division of the Simons Foundation. C.T. acknowledges support by the DFG through the Collaborative Research Center SFB 1143, project A04, the Research Training Group GRK 1621, and the Cluster of Excellence on Complexity and Topology in Quantum Matter ct.qmat (EXC 2147). A.R. acknowledges the financial support of the Swiss National Science Foundation through an Ambizione Grant No. 186043.

[1] C. W. Hicks, M. E. Barber, S. D. Edkins, D. O. Brodsky, and A. P. Mackenzie, Piezoelectric-based apparatus for strain tuning, Rev. Sci. Instrum. **85**, 065003 (2014).

[2] D. O. Brodsky, M. E. Barber, J. A. N. Bruin, R. A. Borzi, S. A. Grigera, R. S. Perry, A. P. Mackenzie, and C. W. Hicks, Strain and vector magnetic field tuning of the anomalous phase in $Sr_3Ru_2O_7$, Sci. Adv. **3**, e1501804 (2017).

[3] J. Park, H. Sakai, O. Erten, A. P. Mackenzie, and C. W. Hicks, Effect of applied orthorhombic lattice distortion on the antiferromagnetic phase of $CeAuSb_2$, Phys. Rev. B **97**, 024411 (2018).

[4] A. E. Böhmer, A. Sapkota, A. Kreyssig, S. L. Bud'ko, G. Drachuck, S. M. Saunders, A. I. Goldman, and P. C. Canfield, Effect of Biaxial Strain on the Phase Transitions of $Ca(Fe_{1-x}Co_x)As_2$, Phys. Rev. Lett. **118**, 107002 (2017).

[5] H.-H. Kim, S. M. Souliou, M. E. Barber, E. Lefrançois, M. Minola, M. Tortora, R. Heid, N. Nandi, R. A. Borzi, G. Garbarino, A. Bosak, J. Porras, T. Loew, M. König, P. J. W. Moll, A. P. Mackenzie, B. Keimer, C. W. Hicks, and M. Le Tacon, Uniaxial pressure control of competing orders in a high-temperature superconductor, Science **362**, 1040 (2018).

[6] D. Sun, D. A. Sokolov, J. M. Bartlett, J. Sannigrahi, S. Khim, P. Kushwaha, D. D. Khalyavin, P. Manuel, A. S. Gibbs, H. Takagi, A. P. Mackenzie, and C. W. Hicks, Magnetic frustration and spontaneous rotational symmetry breaking in $PdCrO_2$, Phys. Rev. B **100**, 094414 (2019).

[7] H. Pfau, C. R. Rotundu, J. C. Palmstrom, S. D. Chen, M. Hashimoto, D. Lu, A. F. Kemper, I. R. Fisher, and Z.-X. Shen, Detailed band structure of twinned and detwinned $BaFe_2As_2$ studied with angle-resolved photoemission spectroscopy, Phys. Rev. B **99**, 035118 (2019).

[8] Y.-T. Hsu, W. Cho, A. F. Rebola, B. Burganov, C. Adamo, K. M. Shen, D. G. Schlom, C. J. Fennie, and E.-A. Kim, Manipulating superconductivity in ruthenates through Fermi surface engineering, Phys. Rev. B **94**, 045118 (2016).

[9] J. Mutch, W.-C. Chen, P. Went, T. Qian, I. Z. Wilson, A. Andreev, C.-C. Chen, and J.-H. Chu, Evidence for a strain-tuned topological phase transition in $ZrTe_5$, Sci. Adv. **5**, eaav9771 (2019).

[10] A. P. Mackenzie, T. Scaffidi, C. W. Hicks, and Y. Maeno, Even odder after twenty-three years: The superconducting order parameter puzzle of Sr_2RuO_4, npj Quantum Mater. **2**, 40 (2017).

[11] C. A. Watson, A. S. Gibbs, A. P. Mackenzie, C. W. Hicks, and K. A. Moler, Micron-scale measurements of low anisotropic strain response of local T_c in Sr_2RuO_4, Phys. Rev. B **98**, 094521 (2018).

[12] A. Steppke, L. Zhao, M. E. Barber, T. Scaffidi, F. Jerzembeck, H. Rosner, A. S. Gibbs, Y. Maeno, S. H. Simon, A. P. Mackenzie, and C. W. Hicks, Strong peak in T_c of Sr_2RuO_4 under uniaxial pressure, Science **355**, eaaf9398 (2017).

[13] M. E. Barber, A. S. Gibbs, Y. Maeno, A. P. Mackenzie, and C. W. Hicks, Resistivity in the Vicinity of a van Hove Singularity: Sr_2RuO_4 under Uniaxial Pressure, Phys. Rev. Lett. **120**, 076602 (2018).

[14] V. Sunko, E. A. Morales, I. Marković, M. E. Barber, D. Milosavljević, F. Mazzola, D. A. Sokolov, N. Kikugawa, C. Cacho, P. Dudin, H. Rosner, C. W. Hicks, P. D. C. King, and A. P. Mackenzie, Direct observation of a uniaxial stress-driven Lifshitz transition in Sr_2RuO_4, npj Quantum Mater. **4**, 46 (2019).

[15] A. Pustogow, Y. Luo, A. Chronister, Y. S. Su, D. A. Sokolov, F. Jerzembeck, A. P. Mackenzie, C. W. Hicks, N. Kikugawa, S. Raghu, E. D. Bauer, and S. E. Brown, Constraints on the superconducting order parameter in Sr_2RuO_4 from oxygen-17 nuclear magnetic resonance, Nature (London) **574**, 72 (2019).

[16] V. Grinenko, S. Ghosh, R. Sarkar, J.-C. Orain, A. Nikitin, M. Elender, D. Das, Z. Guguchia, F. Brückner, M. E. Barber, J. Park, N. Kikugawa, D. A. Sokolov, J. S. Bobowski, T. Miyoshi, Y. Maeno, A. P. Mackenzie, H. Luetkens, C. W. Hicks, and H.-H. Klauss, Split superconducting and time-reversal symmetry-breaking transitions in Sr_2RuO_4 under stress, Nat. Phys. **17**, 748 (2021).

[17] T. M. Rice and M. Sigrist, Sr_2RuO_4: An electronic analogue of ^{3}He? J. Phys.: Condens. Matter **7**, L643 (1995).

[18] C. Kallin and A. J. Berlinsky, Is Sr_2RuO_4 a chiral p-wave superconductor? J. Phys.: Condens. Matter **21**, 164210 (2009).

[19] C. Kallin, Chiral p-wave order in Sr_2RuO_4, Rep. Prog. Phys. **75**, 042501 (2012).

[20] C. Kallin and J. Berlinsky, Chiral superconductors, Rep. Prog. Phys. **79**, 054502 (2016).

[21] J. Xia, Y. Maeno, P. T. Beyersdorf, M. M. Fejer, and A. Kapitulnik, High Resolution Polar Kerr Effect Measurements of Sr_2RuO_4: Evidence for Broken Time-Reversal Symmetry in the Superconducting State, Phys. Rev. Lett. **97**, 167002 (2006).

[22] C. Lupien, W. A. MacFarlane, C. Proust, L. Taillefer, Z. Q. Mao, and Y. Maeno, Ultrasound Attenuation in Sr_2RuO_4: An Angle-Resolved Study of the Superconducting Gap Function, Phys. Rev. Lett. **86**, 5986 (2001).

[23] S. Benhabib, C. Lupien, I. Paul, L. Berges, M. Dion, M. Nardone, A. Zitouni, Z. Q. Mao, Y. Maeno, A. Georges, L. Taillefer, and C. Proust, Ultrasound evidence for a two-component superconducting order parameter in Sr_2RuO_4, Nat. Phys. **17**, 194 (2021).

[24] S. Ghosh, A. Shekhter, F. Jerzembeck, N. Kikugawa, D. A. Sokolov, M. Brando, A. P. Mackenzie, C. W. Hicks, and B. J. Ramshaw, Thermodynamic evidence for a two-component superconducting order parameter in Sr_2RuO_4, Nat. Phys. **17**, 199 (2021).

[25] F. Kidwingira, J. D. Strand, D. J. Van Harlingen, and Y. Maeno, Dynamical superconducting order parameter domains in Sr_2RuO_4, Science **314**, 1267 (2006).

[26] M. S. Anwar, T. Nakamura, S. Yonezawa, M. Yakabe, R. Ishiguro, H. Takayanagi, and Y. Maeno, Anomalous switching in $Nb/Ru/Sr_2RuO_4$ topological junctions by chiral domain wall motion, Sci. Rep. **3**, 2480 (2013).

[27] F. Jerzembeck, H. S. Røising, A. Steppke, H. Rosner, D. A. Sokolov, N. Kikugawa, T. Scaffidi, S. H. Simon, A. P. Mackenzie, and C. W. Hicks, The Superconductivity of Sr_2RuO_4 Under c-Axis Uniaxial Stress, arXiv:2111.06228.

[28] C. W. Hicks, D. O. Brodsky, E. A. Yelland, A. S. Gibbs, J. A. N. Bruin, M. E. Barber, S. D. Edkins, K. Nishimura, S. Yonezawa, Y. Maeno, and A. P. Mackenzie, Strong increase of T_c of Sr_2RuO_4 under both tensile and compressive strain, Science **344**, 283 (2014).

[29] S. Kittaka, S. Nakamura, T. Sakakibara, N. Kikugawa, T. Terashima, S. Uji, D. A. Sokolov, A. P. Mackenzie, K. Irie, Y. Tsutsumi, K. Suzuki, and K. Machida, Searching for gap zeros in Sr_2RuO_4 via field-angle-dependent specific-heat measurement, J. Phys. Soc. Jpn. **87**, 093703 (2018).

[30] E. Hassinger, P. Bourgeois-Hope, H. Taniguchi, S. René de Cotret, G. Grissonnanche, M. S. Anwar, Y. Maeno, N. Doiron-Leyraud, and L. Taillefer, Vertical Line Nodes in the Superconducting Gap Structure of Sr_2RuO_4, Phys. Rev. X **7**, 011032 (2017).

[31] H. G. Suh, H. Menke, P. M. R. Brydon, C. Timm, A. Ramires, and D. F. Agterberg, Stabilizing even-parity chiral superconductivity in Sr_2RuO_4, Phys. Rev. Research **2**, 032023(R) (2020).

[32] A. Ramires and M. Sigrist, Identifying detrimental effects for multiorbital superconductivity: Application to Sr_2RuO_4, Phys. Rev. B **94**, 104501 (2016).

[33] A. Ramires and M. Sigrist, A note on the upper critical field of Sr_2RuO_4 under strain, J. Phys.: Conf. Ser. **807**, 052011 (2017).

[34] A. Ramires, D. F. Agterberg, and M. Sigrist, Tailoring T_c by symmetry principles: The concept of superconducting fitness, Phys. Rev. B **98**, 024501 (2018).

[35] A. Ramires, Nodal gaps from local interactions in Sr_2RuO_4, J. Phys.: Conf. Ser. **2164**, 012002 (2022).

[36] See Supplemental Material at http://link.aps.org/supplemental/10.1103/PhysRevResearch.4.023060 for more information on the derivation of the parameters.

[37] A. Ramires and M. Sigrist, Superconducting order parameter of Sr_2RuO_4: A microscopic perspective, Phys. Rev. B **100**, 104501 (2019).

[38] T. Vogt and D. J. Buttrey, Low-temperature structural behavior of Sr_2RuO_4, Phys. Rev. B **52**, R9843(R) (1995).

[39] M. E. Barber, F. Lechermann, S. V. Streltsov, S. L. Skornyakov, S. Ghosh, B. J. Ramshaw, N. Kikugawa, D. A. Sokolov, A. P. Mackenzie, C. W. Hicks, and I. I. Mazin, Role of correlations in determining the Van Hove strain in Sr_2RuO_4, Phys. Rev. B **100**, 245139 (2019).

[40] P. Blaha, K. Schwarz, G. K. HMadsen, D. Kvasnicka, J. Luitz, R. Laskowsk, F. Tran, L. Marks, and L. Marks, WIEN2k: An Augmented Plane Wave Plus Local Orbitals Program for Calculating Crystal Properties.

[41] J. P. Perdew, K. Burke, and M. Ernzerhof, Generalized Gradient Approximation Made Simple, Phys. Rev. Lett. **77**, 3865 (1996).

[42] N. Marzari and D. Vanderbilt, Maximally localized generalized Wannier functions for composite energy bands, Phys. Rev. B **56**, 12847 (1997).

[43] I. Souza, N. Marzari, and D. Vanderbilt, Maximally localized Wannier functions for entangled energy bands, Phys. Rev. B **65**, 035109 (2001).

[44] J. Kuneš, R. Arita, P. Wissgott, A. Toschi, H. Ikeda, and K. Held, Wien2wannier: From linearized augmented plane waves to maximally localized Wannier functions, Comput. Phys. Commun. **181**, 1888 (2010).

[45] G. Pizzi, V. Vitale, R. Arita, S. Blügel, F. Freimuth, G. Géranton, M. Gibertini, D. Gresch, C. Johnson, T. Koretsune, J. Ibañez-Azpiroz, H. Lee, J.-M. Lihm, D. Marchand, A. Marrazzo, Y. Mokrousov, J. I. Mustafa, Y. Nohara, Y. Nomura, L. Paulatto *et al.*, Wannier90 as a community code: New features and applications, J. Phys.: Condens. Matter **32**, 165902 (2020).

[46] O. Parcollet, M. Ferrero, T. Ayral, H. Hafermann, I. Krivenko, L. Messio, and P. Seth, Triqs: A toolbox for research on interacting quantum systems, Comput. Phys. Commun. **196**, 398 (2015).

[47] P. Giannozzi, S. Baroni, N. Bonini, M. Calandra, R. Car, C. Cavazzoni, D. Ceresoli, G. L. Chiarotti, M. Cococcioni, I. Dabo, A. D. Corso, S. de Gironcoli, S. Fabris, G. Fratesi, R. Gebauer, U. Gerstmann, C. Gougoussis, A. Kokalj, M. Lazzeri, L. Martin-Samos *et al.*, QUANTUM ESPRESSO: A modular and open-source software project for quantum simulations of materials, J. Phys.: Condens. Matter **21**, 395502 (2009).

[48] K. F. Garrity, J. W. Bennett, K. M. Rabe, and D. Vanderbilt, Pseudopotentials for high-throughput DFT calculations, Comput. Mater. Sci. **81**, 446 (2014).

[49] H. Min, J. E. Hill, N. A. Sinitsyn, B. R. Sahu, L. Kleinman, and A. H. MacDonald, Intrinsic and Rashba spin-orbit interactions in graphene sheets, Phys. Rev. B **74**, 165310 (2006).

[50] M. Sigrist and K. Ueda, Phenomenological theory of unconventional superconductivity, Rev. Mod. Phys. **63**, 239 (1991).

[51] A. Tamai, M. Zingl, E. Rozbicki, E. Cappelli, S. Riccò, A. de la Torre, S. McKeown Walker, F. Y. Bruno, P. D. C. King, W. Meevasana, M. Shi, M. Radović, N. C. Plumb, A. S. Gibbs, A. P. Mackenzie, C. Berthod, H. U. R. Strand, M. Kim, A. Georges, and F. Baumberger, High-Resolution Photoemission on Sr_2RuO_4 Reveals Correlation-Enhanced Effective Spin-Orbit Coupling and Dominantly Local Self-Energies, Phys. Rev. X **9**, 021048 (2019).

[52] H.-H. Klauss (private communication).

[53] S. A. Kivelson, A. C. Yuan, B. Ramshaw, and R. Thomale, A proposal for reconciling diverse experiments on the superconducting state in Sr_2RuO_4, npj Quantum Mater. **5**, 43 (2020).

[54] A. W. Lindquist and H.-Y. Kee, Distinct reduction of Knight shift in superconducting state of Sr_2RuO_4 under uniaxial strain, Phys. Rev. Research **2**, 032055(R) (2020).

[55] Y. Yu, A. K. C. Cheung, S. Raghu, and D. F. Agterberg, Residual spin susceptibility in the spin-triplet orbital-singlet model, Phys. Rev. B **98**, 184507 (2018).